Non-Covalent Calixarene–Amino Acid Complexes Formed by MALDI-MS

Michele M. Stone, Andreas H. Franz, and Carlito B. Lebrilla
Department of Chemistry, University of California, Davis, Davis, California, USA

Non-covalent inclusion complexes formed between amino acids and derivatized calix[6]arenes are observed in MALDI mass spectrometry. The methyl, ethyl, and propyl ester derivatives of calix[6]arene yielded amino acid complexes, while the smaller calix[4]arene analogs did not. Similarly the underivatized calix[6]arene and calix[4]arene did not produce complexes. Amino acid complexes were observed for nearly all 20 amino acids in time-of-flight (TOF) analysis. In Fourier transform mass spectrometry (FTMS) analysis, however, only the most basic amino acids arginine, histidine, and lysine formed stable adducts. The complexes were abundant under matrix-assisted laser desorption ionization (MALDI) conditions, which suggested favorable interactions between host and guest. (J Am Soc Mass Spectrom 2002, 13, 964–974)
© 2002 American Society for Mass Spectrometry

Calixarenes owe their utility to their ability to act as host compounds, forming host–guest complexes in solution [1–3]. Their applications in this function are diverse. The high selectivity of some calixarenes for cesium and uranium-containing ions has led to their use in nuclear waste treatment [1, 2, 4]. The selectivity of others for smaller alkali metals has led to their studies as sensor devices [5–9]. In some instances, calixarenes were also used as catalysts in synthetic reactions [10–13] and as liquid crystals [14].

Calixarenes share structural similarities with crown ethers and cyclodextrins—compounds used extensively for molecular recognition. However, calixarenes possess sizable inner "cavities" that crown ethers or their derivatives do not. In addition, they are synthetically prepared allowing a wider array of sizes and shapes that are not available with cyclodextrins.

By far the majority of the studies that involve calixarenes center around the recognition of ionic metal species. Investigations that explore the use of calixarenes for amino acid recognition are less common [15–20]. They are smaller in number than similar studies with cyclodextrins, which also form inclusion complexes with organic amines. However, the potential of calixarenes as artificial receptors and sensors for biomolecules, specifically amino acids and peptides, has long been recognized. The vast majority of these studies on calixarenes has focused on the calix[4]arenes, primarily because they possess open and rigid structures that are desirable for molecular recognition [3, 21, 22]. Arena et al. examined the complexation of a number of naturally occurring amino acids with soluble derivatives of calix[4]arenes [23]. The host compounds were derivatized with carboxylic acids and sulfate esters. Calix[4]arenes derivatized with α-aminophosphonates were found to exhibit high selectivity as carriers of the zwitterionic forms of aromatic amino acids through membranes [18]. In chromatography, silica-bonded calixarenes have been used for retaining amino acid esters [24]. Chiral recognition of α-amino acids by calixarenes has also been investigated [25, 26].

Gas-phase complexes of calixarenes are readily produced by a number of ionization methods [27–30]. Calixarenes are intrinsically strong chelators of alkali metal ions and produce the corresponding quasimolecular ions abundantly. Metal binding selectivites of a series of calixarenes have been determined by Brodbelt and co-workers using matrix-assisted laser desorption/ionization (MALDI) and electrospray ionization (ESI). Size selectivities were obtained with various derivatized compounds [31, 32]. Complexes of calix[4]arenes with alkylammonium ions have been generated directly from solution by ESI [33]. The complex of calix[4]arene with benzylammonium cation has been generated by Dearden and co-workers by gas-phase ion molecule reactions [34]. Similar reactions have been used extensively by Vincenti and co-workers to produce a number of gas-phase host–guest complexes [27, 35, 36]. A number of higher order complexes composed of guest molecules sequestered in multiple calixarene hosts (usually 2:1 host/guest) has been produced using electrospray ionization.

The gas-phase chemistry of calixarene-amino acid complexes may provide indications of the intrinsic utility of calixarenes as recognition devices for amino acids and peptides. However, to date, there have been no reported studies of these complexes in the gas-phase.

Published online June 25, 2002
Address reprint requests to Dr. C. B. Lebrilla, Department of Chemistry, University of California, Davis, One Shields Avenue, Davis, CA 95616, USA. E-mail: cblebrilla@ucdavis.edu

© 2002 American Society for Mass Spectrometry. Published by Elsevier Science Inc.
1044-0305/02/$20.00
PII S1044-0305(02)00417-8
Received April 1, 2002
Accepted April 3, 2002

In this report, we show that modified calix[6]arene binds strongly to amino acids to produce gas-phase complexes that withstand even the relatively energetic process of MALDI. The formation of these complexes, particularly by MALDI, is unprecedented. No host–guest complexes of either cyclodextrins or crown ethers have been produced in the gas phase by this ionization method. This attests to the strength of the interactions in the complex.

Experimental

Unless stated otherwise, the chemicals used in the derivatization reaction were purchased from Sigma-Aldrich (St. Louis, MO) and used without further purification. Amino acids were purchased from Research Plus, Inc. (Denville, NJ) and Sigma Chemical Company (St. Louis, MO). Solvents were of HPLC grade.

Fourier Transform Ion Cyclotron Resonance (FT-ICR) mass spectra were recorded on an external source HiResMALDI (IonSpec Corporation, Irvine, CA) equipped with a 4.7 Tesla magnet and a LSI 337-nm nitrogen laser. TOF data was recorded using a Proflex III MALDI-TOF instrument (Bruker-Daltonics, Billerica, MA) with a 337 nm nitrogen laser. 2,5-Dihydroxybenzoic acid (DHB, 5 mg/100 μL in ethanol) was used as the matrix in all experiments. An ammonium-resin was used to desalt the calixarene solutions and produce the NH_4^+ adduct. Amino acid solutions were prepared at a concentration of 100 mg/mL in water. For the amino acids not soluble at this concentration, the saturated solution was used.

Preparation of the Ammonium Resin

The cation exchange resin (ammonium form) was prepared by a previously published procedure [37]. An H^+ cation exchange resin (100–200 mesh, Bio-Rad, NY) was stirred in a 1 M ammonium acetate solution for 12 h. The product was filtered and washed with 1 M ammonium acetate solution, deionized water, acetone, and hexane. The resin was dried and stored for future use.

Synthesis of Modified Calixarenes

The modified calix[4] and calix[6]arenes (Scheme **1**) were all synthesized using the same procedure. The procedure for calix[6]arene hexaethyl ester (**C6A-Et**) is provided and was modified from the method published by Arnaud-Neu et al. [38] and Grady et al. [39] Calix[6]arene (**C6A**, 200 mg, 0.31 mmol) was suspended in dry acetone (5 mL). Anhydrous potassium carbonate (390 mg, 2.82 mmol, 50% molar excess over 6 OH-groups) was added at room temperature followed by ethyl bromoacetate (0.4 mL, 3.77 mmol, 100% molar excess over 6 OH-groups). The reaction mixture was heated to reflux for 12 h under exclusion of moisture, cooled to room temperature, and allowed to sit overnight. Thin layer chromatography (TLC) on silica gel (solvent: $CHCl_3$) showed complete consumption of the starting material. The reaction mixture was filtered through Celite (J. T. Baker, Phillipsburg, NJ). The KBr filter cake was washed with $CHCl_3$ (3 $\times$ 5 mL). The combined organic filtrates were evaporated to dryness on a rotavap (model R-3000, Büchi, New Castle, DE) in vacuo ($\sim 10^{-4}$torr) and the residue was crystallized twice from ethanol to give the hexaethyl ester (**C6A-Et**).

Synthesis of the Hexamethyl and Hexapropyl Ester of Calix[6]Arene

C6A-Et (0.4 g, 0.35 mmol) was suspended in a solution of ethanol:water (1:1, 10 mL) and potassium hydroxide (0.4 g, 7 mmol) was added. The mixture was heated to reflux for 2 h and cooled to room temperature. Addition of concentrated hydrochloric acid to pH = 1 gave a white precipitate, which was filtered off. The product was suspended in water (10 mL) and potassium hydroxide (0.4 g, 7 mmol) was added. The mixture was heated to reflux for another 5 h and cooled to room temperature. Addition of concentrated hydrochloric acid to pH = 1 gave a white precipitate, which was filtered off and dried over $CaCl_2$ in an evacuated desiccator (yield: 87%). The free acid (1 mg, 1 mmol) was dissolved in thionyl chloride (30 μL) and heated to 60 °C for 1 h. To this solution methanol (100 μL) or n-propanol (100 μL) was added slowly to give **C6A-Me** and **C6A-nPr**, respectively. Subsequently, the solution in $CHCl_3$ was filtered through a small plug of aluminum oxide (basic, activated, Brockman I) to remove any free acid.

Mass Spectrometric Analysis (MALDI-FT-ICR)

The derivatized calixarenes were dissolved in chloroform (c $\sim 10^{-5}$ M). The resulting solution (1 μL) was applied to the MALDI probe along with a small amount of ammonium-resin, followed by amino acid solution (1 μL, 100 mg/mL) and matrix solution (2 μL). The samples were crystallized under a stream of air and subjected to mass spectral analysis [40–43]. The standard FT-ICR pulse sequence consisted of a laser pulse, a gas pulse (argon) after 100 ms to cool the ions, and detection after 5000 ms. For all CID experiments, the appropriate isolation pulses were programmed starting at 3 s after the initial ionization and were followed by sustained off resonance irradiation (SORI) excitation at 6 s (1 s, 5 V base to peak, +1000 Hz off-resonance). At a background pressure of 10^{-10} torr, argon gas was administered through a pulse valve at 6 and at 6.5 s for 2 ms each to generate a peak pressure of $5 * 10^{-5}$ torr. Final excitation for detection was performed 12 s after the initial laser pulse.

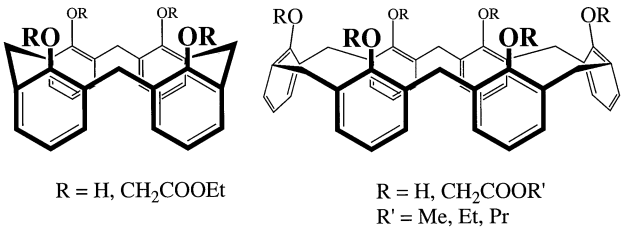

Scheme 1 Chemical structures of the investigated calixarenes.

Mass Spectrometric Analysis (MALDI-TOF)

The calixarene solution (0.5 μL) was applied to the MALDI probe along with a small amount of ammonium-resin, followed by amino acid solution (0.5 μL) and matrix solution (1 μL). The samples were crystallized under a stream of air and subjected to mass spectral analysis. Ion lens 1 was charged to 20 kV. The voltage on the second ion extraction lens was adjusted for optimal focussing (18.60–19.10 kV). The laser discharge frequency was 2 Hz with a detector time window of 1 ns corresponding to an *m/z* window of 4500.

Molecular Modeling

Calculations were performed using Biosym Insight II with the consistent valence force field (CVFF). Calculations of the complexes were started with fully optimized calixarene host and amino acid structures. During the simulation, the structures of both the amino acids and the hosts were allowed to fully optimize. Unless stated otherwise, the complex was heated to 600 K for 400 ps. At every 8 ps, a structure from the trajectory was captured and annealed in steps of 100 to 0 K. The heating/annealing cycles helped to avoid local minima and facilitated finding the global minimum. This resulted in 50 annealing simulations with a corresponding number of structures.

Results

MALDI-FT-ICR of Calix[4]arene and Calix[6]arene

MALDI-FT-ICR analysis of the calix[4]arene (R = H, Scheme **1**) produced the alkali metal ion adducts. For example, the sodiated species (*m/z* 447.173) yielded a high signal-to-noise ratio (Figure 1a). Alkali metal coordinated species were also abundant for calix[6]arene (**C6A** R = H, Scheme **1**). For example, the FTMS of **C6A** produced the sodiated species (*m/z* 659.243) when the sample was doped with NaCl (Figure 1b), with little fragmentation observed. The signal at *m/z* 715.310 was due to an impurity. An impurity due to calix[5]arene gave the signal at *m/z* 553.202. When the compound was doped with other alkali metal salts, the corresponding alkali metal coordinated species were observed as the major peak in the MALDI-MS spectra. MALDI-TOF spectra produced similarly strong signals of the quasi-

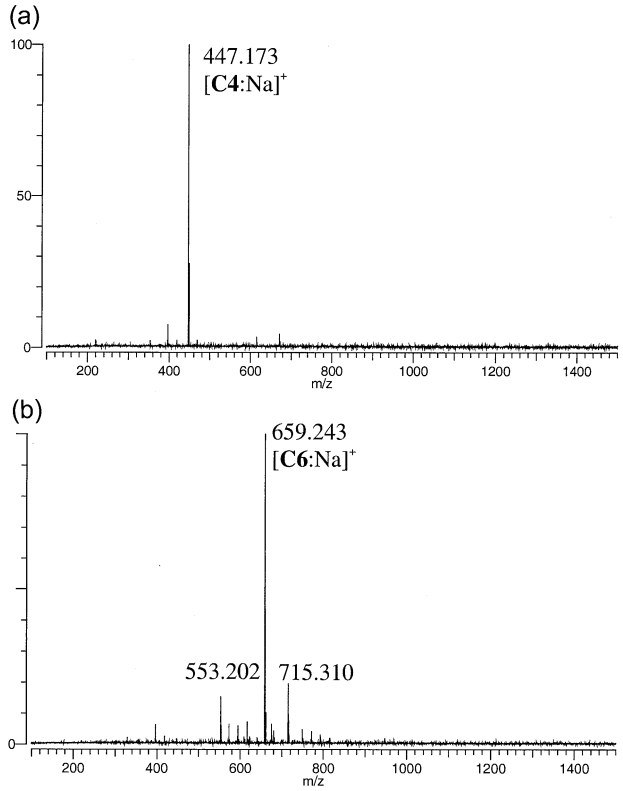

Figure 1. (**a**) MALDI-FTMS spectrum of native calix[4]arene doped with sodium (*m/z* 447.173); (**b**) MALDI-FTMS spectrum of native calix[6]arene doped with sodium (*m/z* 659. 243). The signal at *m/z* 715.310 was due to an impurity.

molecular ion with high signal-to-noise. Calixarenes are structurally similar to crown ethers, which are also known to be strong chelators of alkali metal ions in the solution-phase [34]. Indeed, both the calix[4]arene and calix[6]arene produced abundant quasimolecular ions with all alkali metals attempted (Li^+, K^+, Rb^+, Cs^+, data not shown).

Attempts to produce the ammonium coordinated species of the underivatized parent compounds failed despite numerous attempts including varying the sample preparation conditions and the solvents. Only the sodium and potassium coordinated species were observed when the sample was exposed to ammonium-resin (spectra not shown). Potassium and sodium are common contaminants and typically coordinate to polyoxygenated compounds.

MALDI-MS of Derivatized Calix[6]arene

The derivatives of calix[6]arene were prepared with R = $CH_2CO_2CH_3$ (**C6A-Me**), R = $CH_2CO_2CH_2CH_3$ (**C6A-Et**), and R = $CH_2CO_2CH_2CH_2CH_3$ (**C6A-Pr**) as described in the experimental method section. The FT-ICR mass spectra of the esters of calix[6]arene doped with alkali metal salts produced the corresponding quasimolecular ions as the most abundant peaks. The quality of the spectra was similar to those shown in Figure 1.

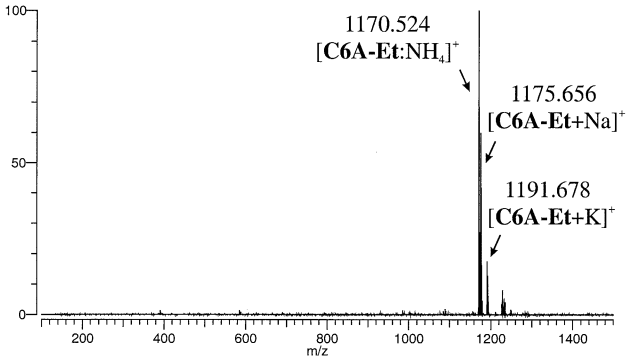

Figure 2. MALDI-FTMS spectrum of **C6A-Et** in the presence of ammonium-resin. The ammonium, sodium and potassium adducts were observed in high abundance.

Addition of the amino acids directly to the calixarene samples did not produce the calixarene-amino acid complex. However, when the derivatized calix[6]arenes were exposed to ammonium resin on the probe tip, the ammonium complexes were observed. For example, the MALDI-FTMS of **C6A-Et** yielded the spectra shown in Figure 2. The major peaks at *m/z* 1170.524, 1175.656, and 1191.678 are the NH_4^+ ([**C6A-Et**:NH_4]$^+$), the Na^+ ([**C6A-Et**:Na]$^+$), and the K^+ ([**C6A-Et**:K]$^+$) adducts, respectively. Minor peaks at *m/z* 1228.531 and 1233.689 (not labeled) were due to impurities.

We subsequently investigated ethylamine, propylamine, ethylenediamine, and 1,3-di-aminopropane as guest molecules. Representative spectra obtained under identical experimental conditions are shown in Figure 3. Ethyl amine in Figure 3a yielded the adduct peak [**C6A-Et**:$EtNH_3$]$^+$ at *m/z* 1198.755 (52% relative to [**C6A-Et**:NH_4]$^+$). Propyl amine (spectrum not shown) gave rise to [**C6A-Et**:$PrNH_3$]$^+$ at *m/z* 1212.784 (25% relative to [**C6A-Et**:NH_4]$^+$). The di-amino compounds ethylene diamine (Figure 3b) and 1,3-di-amino propane (spectrum not shown) yielded [**C6A-Et**:EDA + H]$^+$ at *m/z* 1214.683 (6% relative to base peak [**C6A-Et**:Na]$^+$) and [**C6A-Et**:1,3DAP + H]$^+$ at *m/z* 1227.639 (8% relative to base peak [**C6A-Et**:Na]$^+$), respectively. The ammonium adduct [**C6A-Et**:NH_4]$^+$ was not observed with the di-amino compounds.

We obtained a similar result with guests such as guanidine. Spectra obtained with guanidinium hydrochloride and creatinine sulfate are shown in Figure 4. Guanidine and creatinine revealed no significant abundance of [**C6A-Et**:Na]$^+$ in their spectra, respectively. Guanidine (G) yielded a strong signal for [**C6A-Et**:G + H]$^+$ at *m/z* 1212.645 (137% relative to [**C6A-Et**:NH_4]$^+$). Creatinine (C) formed an adduct [**C6A-Et**:C + H]$^+$ at *m/z* 1266.576 (23% relative to [**C6A-Et**:NH_4]$^+$). The high abundance of the guanidine-**C6A-Et** adduct pointed towards a favorable interaction between the guest ion and the calixarene host.

The successful formation of gas-phase adducts between ammonium/guanidinium compounds and **C6A-Et** prompted us to investigate amino acids as guest

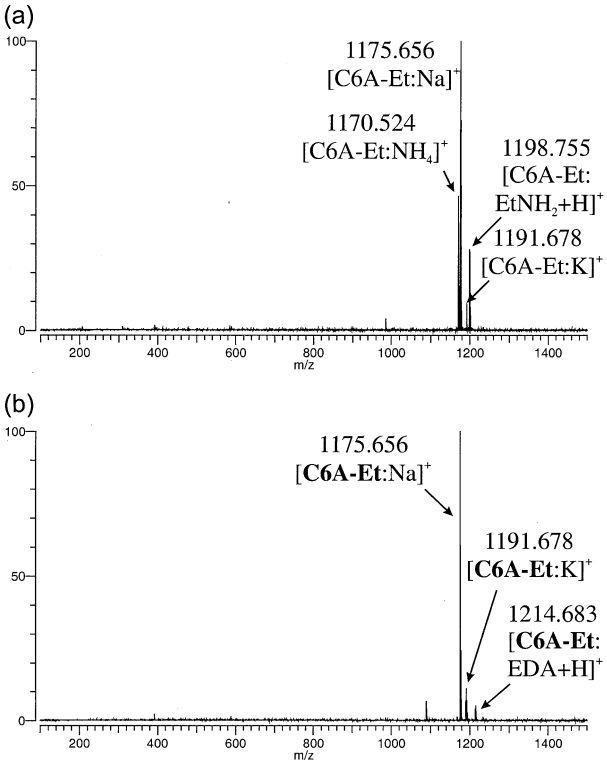

Figure 3. (**a**) MALDI-FTMS spectrum of **C6A-Et** in the presence of ammonium-resin and ethyl amine; (**b**) MALDI-FTMS spectrum of **C6A-Et** in the presence of ammonium-resin and ethylene diamine.

ions. Addition of the amino acid lysine (Lys) to the resin-exposed sample followed by MALDI-FTMS analysis yielded the spectrum in Figure 5. The presence of the peak at *m/z* 1299.788 corresponded to a calixarene-amino acid adduct ([**C6A-Et**:Lys + H]$^+$) (Figure 5). To obtain spectra with appreciable intensities of the adduct, the calixarene solution was also mixed with ammonium-resin prior to MALDI analysis. The resin facilitated the production of the ammonium and amino acid complexes. Without the resin only the Na^+ and K^+ adduct peaks were observed.

A systematic study involving 20 naturally occurring amino acids was performed in both TOF and FTMS to determine the effect of amino acid size and gas-phase basicity on complex formation. Table 1 summarizes the results of these experiments for both the FTMS and the TOF instruments. The amino acids were arranged in order of increasing gas-phase basicity. For each amino acid, the intensity of the **C6A-Et**-amino acid complex was given as percent relative to the NH_4^+ adduct (base peak).

With the FTMS analyzer only the three most basic amino acids, namely His, Lys, and Arg, were observed to produce the complex. However, the MALDI-FTMS result of **C6A-Et** with valine was representative of amino acids that did *not* form complexes with **C6A-Et** (spectrum not shown). The ammonium complex (*m/z* 1170.524) was the most abundant ion followed by the

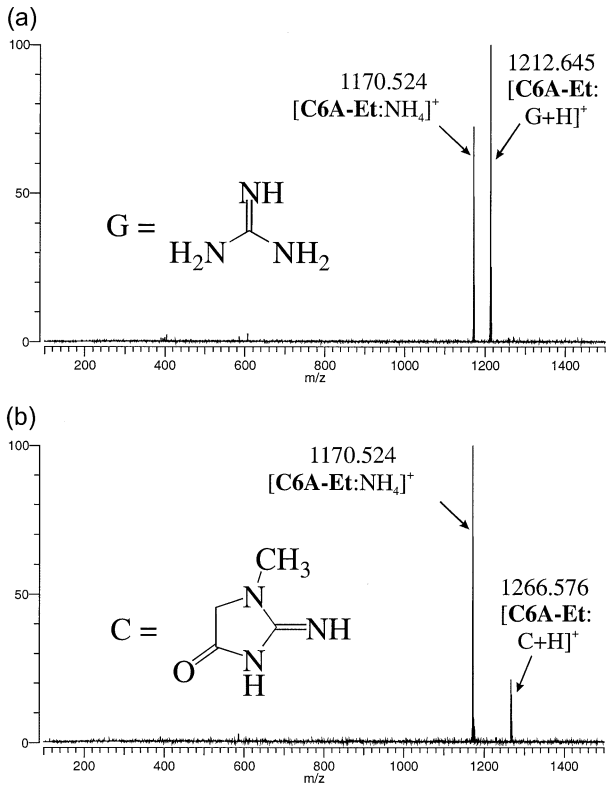

Figure 4. (**a**) MALDI-FTMS spectrum of **C6A-Et** in the presence of ammonium-resin and guanidinium hydrochloride; (**b**) MALDI-FTMS spectrum of **C6A-Et** in the presence of ammonium-resin and creatinine sulfate.

Na^+ (*m/z* 1175.656) and the K^+ (*m/z* 1191.678) complexes.

For comparison, similar studies were performed with MALDI-TOF. The detection times vary considerably between TOF and FTMS allowing metastable phenomena to be observed. Figure 6a and b show the [**C6A-Et**:Arg + H]$^+$ (*m/z* 1328.2) and [**C6A-Et**:Lys + H]$^+$ (*m/z* 1300.2) complexes. In the time-of-flight mass analyzer, nearly all the amino acids formed complexes with **C6A-Et** except for glycine, the least basic amino acid, and cysteine. Furthermore, the relative intensity of the complex peak increased with increasing amino acid basicity. As in the FT-ICR experiments, the ammonium-coordinated species were the most abundant. Similarly, the three most basic amino acids, Arg, Lys, and His, gave the most abundant adducts. However, MALDI-TOF produced more complexes with the amino acids than MALDI-FT-ICR.

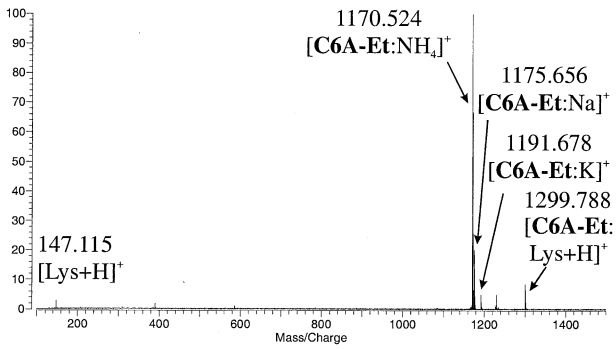

Figure 5. MALDI-FTMS spectrum of **C6A-Et** in the presence of ammonium-resin and lysine.

That the amino acid complexes were obtained in both mass spectrometers attested to the strength of the interaction. However, because of the different time scales between the two techniques, complexes that were observed in the TOF analyzer may not be observed in the FTMS, particularly if the complexes are metastable to a certain extent. The presence of the complexes in the FTMS indicated that they were sufficiently long-lived and were stable under ambient conditions.

The relatively high abundance of calixarene–amino acid complexes prompted us to investigate the behavior of those complexes during collision-induced dissociation (CID) experiments. CID experiments of the Arg, Lys and His adducts were performed in the FTMS instrument to determine whether the complexes were truly non-covalent. Figure 7a shows the MALDI-FTMS spectrum of the arginine-doped **C6A-Et**. The complex peak [**C6A-Et**:Arg + H]$^+$ at *m/z* 1327.604 is approximately 60% relative to the ammonium coordinated species. The isolation (Figure 7b) and subsequent CID of the complex yielded only protonated Arg (Figure 7c). Fragmentation of **C6A-Et** was not observed to a significant extent. Note the presence of the protonated arginine at *m/z* 175.121 in the MALDI-FTMS spectrum (Figure 7a). In our experimental setup, ions below *m/z* 300 are not generally transmitted through the quadrupole ion guide. Therefore, the presence of protonated arginine indicated that the complex underwent metastable decay in the ICR cell prior to detection.

MALDI-MS Competition Studies of Amino Acids with Calix[6]arene Derivatives

We investigated subsequently the selectivity of **C6A-Me**, **C6A-Et**, and **C6A-Pr** towards arginine, histidine, and lysine. Addition of equal amounts of amino acids to **C6A-Me** yielded the arginine adduct [**C6A-Me**:Arg + H]$^+$ at *m/z* 1243.548 formed with 40% abundance relative to the ammonium adduct at *m/z* 1086.436 (spectra not shown). The histidine adduct [**C6A-Me**:His + H]$^+$ at *m/z* 1224.507 formed in only 2% abundance relative to the ammonium adduct while the lysine adduct was not detected. Similar results were obtained with **C6A-Et** and **C6A-Pr**. For all three hosts, the respective ariginine complexes formed in 40% (*m/z* 1243.548), 27% (*m/z* 1327.604), and 13% (*m/z* 1411.691) abundances, respectively (spectra not shown). These results suggested that steric factors may destabilize complexes with larger alkyl groups on the calixarene. In all cases, the arginine adducts were significantly more abundant than the histidine complexes, which were produced in trace abundance. The lysine adducts were not detected.

Table 1. Comparison of complex formation between **C6A-Et** and amino acids of TOF and ICR detectors. The complex formation is given in percent relative to [**C6A-Et**:NH_4]$^+$

Amino Acid		Molecular mass	Complex mass	Complex (ICR)	Complex (TOF)	GB (kJ/mol)
Glycine	Gly	75.07	1229.1	0	0	852.2
Alanine	Ala	89.09	1243.1	0	2	867.7
Cysteine	Cys	121.2	1275.2	0	0	869.3
Aspartic acid	Asp	133.1	1287.1	0	2	875
Valine	Val	117.2	1271.2	0	3	876.7
Glutamic acid	Glu	147.1	1301.1	0	4	879.1
Leucine	Leu	131.2	1285.2	0	5	880.6
Serine	Ser	105.1	1259.1	0	4	880.7
Isoleucine	Ile	131.2	1285.2	0	4	883.5
Proline	Pro	115.1	1269.1	0	5	886
Threonine	Thr	119.1	1273.1	0	1	888.5
Phenylalanine	Phe	165.2	1319.2	0	6	888.9
Asparagine	Asn	132.1	1286.1	0	3	891.5
Tyrosine	Tyr	181.2	1335.2	0	5	892.1
Glutamine	Gln	146.1	1300.1	0	5	900
Methionine	Met	149.2	1303.2	0	2	901.5
Tryptophan	Trp	204.2	1358.2	0	6	915
Histidine	His	155.2	1309.2	31	10	950.2
Lysine	Lys	146.2	1300.2	15	10	951
Arginine	Arg	174.2	1328.2	12	14	1007

MALDI-MS of Derivatized Calix[4]arene

The behavior of the calix[4]arene derivatives contrasted with that of the calix[6]arene for the amino acids. As with calix[6]arene, the alkali metal coordinated species were produced in great abundances with both MALDI-FTMS and MALDI-TOF. However, under the same conditions and sample treatment as that used with calix[6]arene derivatives, ammonium complexes were not observed. For the ethyl ester of calix[4]arene (**C4A-Et**), only the Na^+ (*m/z* 791.299) and K^+ coordinated species (*m/z* 825.264) were observed with the Na^+ adduct in significantly greater abundance (spectrum not shown). The resin treatment did not yield the ammonium complex [**C4A-Et**:NH_4]$^+$. Similarly, the direct addition of the amino acid or the resin pretreatment did not yield complexes for any of the amino acids.

Molecular Modeling of Calixarene Complexes

The nature of the interaction between the amino acids and the calixarene **C6A-Et** was examined with molecular modeling. Several different initial conformations of the **C6A-Et** host molecule were considered for complex formation. The substitution on the lower rim of **C6A-Et** prevented ring-through-the-annulus rotation of the ester groups during the annealing process. However, the lack of substitution on the upper rim made ring-through-the-annulus rotation of the aromatic hydrogens possible. For example, inclusion complexes of **C6A-Et** with alkali metal cations were favored by conformers with ring-through-the-annulus rotation of at least one aromatic ring (results not shown). With the amino acids, however, only the complexes formed with the winged-cone conformation as shown in Figure 8 were stable during the temperature annealing process.

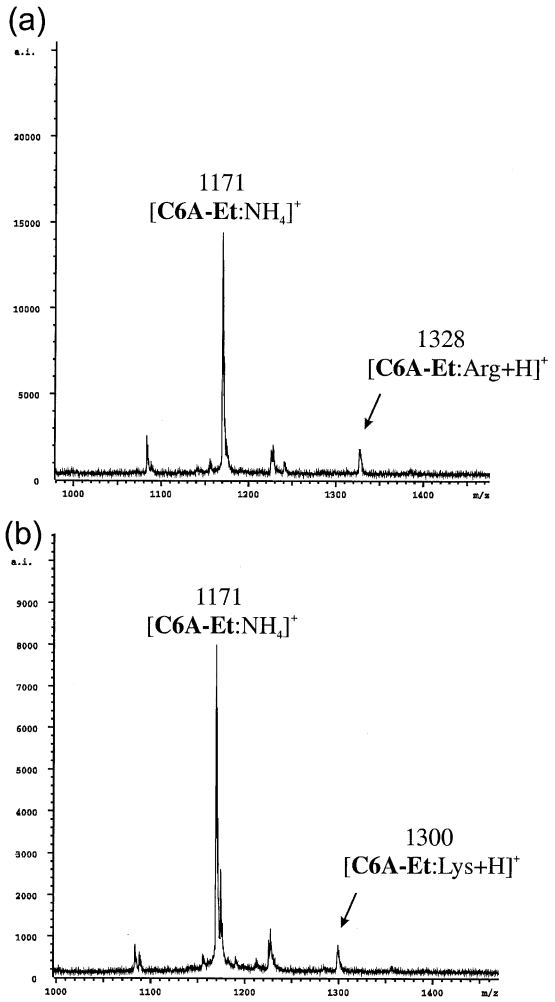

Figure 6. (**a**) MALDI-TOF spectrum of **C6A-Et** in the presence of ammonium-resin and arginine; (**b**) MALDI-TOF spectrum of **C6A-Et** in the presence of ammonium-resin and lysine.

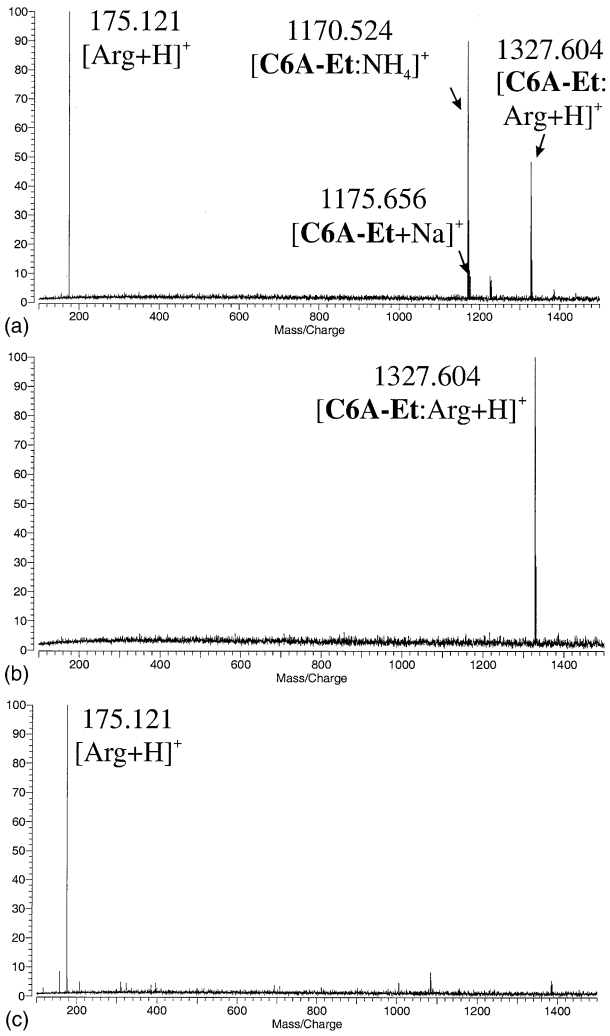

Figure 7. (**a**) MALDI-FTMS spectrum of **C6A-Et** in the presence of ammonium-resin and arginine; (**b**) isolated complex ion of [**C6A-Et**:Arg + H]$^+$; (**c**) CID spectrum of [**C6A-Et**:Arg + H]$^+$. Only protonated arginine at *m/z* 175.121 was observed without significant fragmentation of the host.

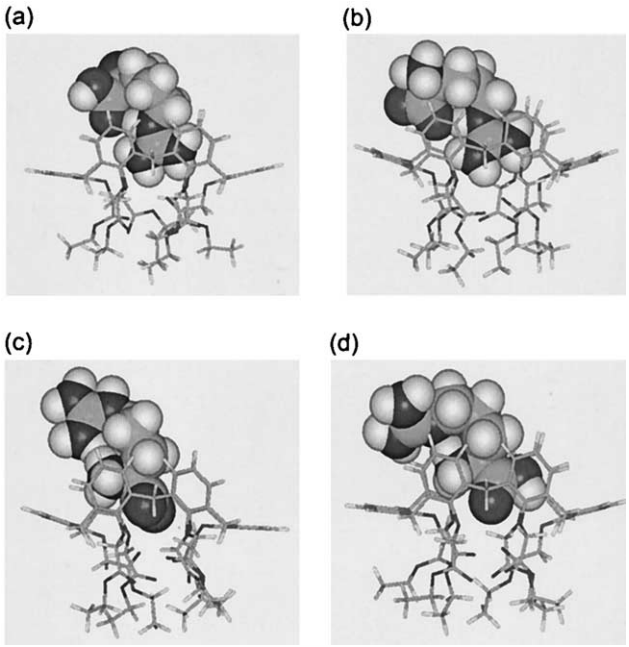

Figure 8. (**a**) Lowest energy structure of T1, protonation on the guanidine group with neutral amine and carboxylic acid group; (**b**) lowest energy structure of T2, protonation on the guanidine group and a zwitterion formed between the N-terminus and the carboxylic acid (guanidinium inside the cavity); (**c**) lowest energy structure of T3, protonation on the guanidine group and a zwitterion formed between the N-terminus and the carboxylic acid (zwitterion inside the cavity); (**d**) lowest energy structure of T4, protonation on the N-terminus with neutral guanidine and carboxylic acid groups. The structures were obtained by molecular dynamics simulation with temperature annealing starting at 600 K.

We investigated complexes of ammonium, protonated valine, and protonated arginine with **C6A-Et**. The complexes of protonated arginine [**C6A-Et**:Arg + H]$^+$ proved to be stable and withstood the annealing cycle typically employed to find the lowest conformations. This method involved heating the complex at 600 K for several ps. Three tautomers of protonated arginine, with four different modes of interaction with the calixarene host, were examined: (T1) protonation on the guanidine group with neutral amine and carboxylic acid group, (T2) protonation on the guanidine group and a zwitterion formed between the N-terminus and the carboxylic acid (guanidinium inside the cavity), (T3) protonation on the guanidine group and a zwitterion formed between the N-terminus and the carboxylic acid (zwitterion inside the cavity), and (T4) protonation on the N-terminus with neutral guanidine and carboxylic acid groups.

The complex T1 was calculated to yield the structure shown in Figure 8a. In the gas-phase, this species yielded a total energy of +38.8 kcal/mol relative to the most stable structure T4. The guanidinium unit was buried deep inside the host cavity because of hydrogen bonding with the phenolic oxygens and π-interactions with the aromatic rings. The shortest distance between the hydrogens of the guanidinium group and the two phenolic oxygens on the "wings" of the aromatic ring system was 2.3 Å. The guanidinium hydrogens and the other four phenolic oxygens were separated by at least 4.5 Å. The shortest distances between the hydrogens of the guanidinium group and the aromatic carbon atoms (proton-π interactions) were 3.2–4.0 Å. Intramolecular hydrogen bonding between the guanidinium hydrogen closest to the carbonyl oxygen of the acid terminus appeared strong with a bond distance of only 1.87 Å.

Figure 8b shows the result of the calculation with T2. The guanidinium group remained inside the cavity of **C6A-Et**. The shortest distance between the guanidinium hydrogens and the phenolic oxygens on both wings of the host was 2.2 Å. Additional hydrogen bonding—the shortest distance being 2.88 Å— was observed between those hydrogens and the ester carbonyl oxygens on the wings. Proton-π interactions were similar to T1 with the shortest distance between the guanidinium hydrogens and the aromatic carbon atoms being 3.3–4.0 Å. The

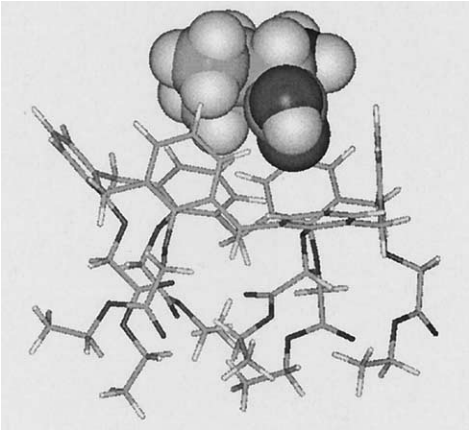

Figure 9. Lowest energy structure of [**C6A-Et**:Val + H]$^+$ determined by molecular dynamics simulation with temperature annealing starting at 300 K.

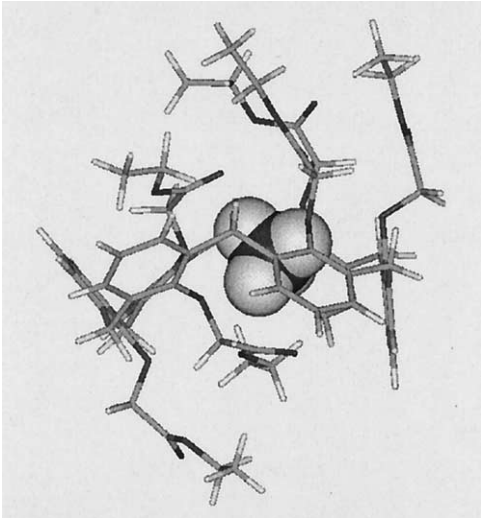

Figure 10. Lowest energy structure of [**C6A-Et**:NH_4]$^+$ determined by molecular dynamics simulation with direct minimization.

intramolecular hydrogen bonding between the carboxylate and the guanidinium hydrogen was also apparent with a distance of only 1.75 Å. The arginine structure was effectively characterized by a salt bridge with the interactions guanidinium-carboxylate-ammonium. The total energy for the structure as shown was +28.5 kcal/mol relative to T4.

The lowest energy structure for T3 is shown in Figure 8c. The amino acid termini were in zwitterioinic form and remained inside the host molecule. Hydrogen bonding was observed between the protons of the ammonium group and the phenolic oxygen on the wing. The shortest distance was 2.79 Å. Proton-π interactions appeared stronger with bond distances of 2.5–4.0 Å between the ammonium hydrogens and the aromatic carbon atoms. With a relative total energy of +30.0 kcal/mol T3 was energetically equivalent to T2.

The tautomer T4 yielded the structure shown in Figure 8d. The protonated amino acid terminus was buried deep inside the **C6A-Et** host. Stabilizing hydrogen bonding was observed between the ammonium hydrogens and the phenolic wing oxygen (2.3 Å) on the one side and the carboxylic acid hydrogen and the phenolic wing oxygen (2.0 Å) on the other side. Hydrogen bonding between the neutral guanidine and the ammonium hydrogens was exceptionally strong with a bond distance of only 1.86 Å. Proton-π interactions between the ammonium hydrogens and the phenyl rings yielded bond distances of 3.3–4.5 Å. Based on the molecular structure it was not immediately apparent why T4 resulted in the lowest energy for a [**C6A-Et**:Arg + H]$^+$ complex.

The valine complex [**C6A-Et**:Val + H]$^+$ could not be annealed at this temperature and promptly dissociated. However, the valine complex was found to be stable at 300 K for 400 ps. The resulting lowest energy structure is shown in Figure 9 with the protonated amino acid inside the host cavity. The carboxylic acid group weakly interacted with the phenolic oxygens to form a stabilizing hydrogen bond. The shortest distance between the carboxylic acid hydrogen and the phenolic oxygens was 4.0 Å. The distance between the ammonium hydrogens and the aromatic ring carbons (proton-π interactions) was 2.9–4.7 Å. The observed distances for stabilizing hydrogen bonds or proton-π interactions were significantly longer and less numerous than observed for the arginine complexes [**C6A-Et**:Arg + H]$^+$.

The ammonium complex [**C6A-Et**:NH_4]$^+$ could not be temperature annealed at 300 K. Figure 10 shows the lowest energy structure that we obtained with simple minimization. Initiating the calculation with the winged cone of the host molecule—used previously for the amino acid complexes—proved unsuitable for the stabilization of the ammonium complex even under simple minimization conditions. A stable complex was obtained when NH_4^+ was fully encapsulated as shown in Figure 10. Hydrogen bonding with the phenolic oxygens stabilized the guest ion. For all four ammonium hydrogens bond distances of 2.1–2.9 Å were observed. In addition, the ester side chains formed "lids" on both sides of the cavity. This steric interaction helped to keep the ammonium ion inside the host molecule.

Discussion

The results from molecular modeling were generally consistent with the experimental results. The valine complex was not observed in the ICR-cell but was observed in the TOF analyzer with only low abundance (Table 1). The arginine complex, on the other hand, was abundant and readily observed with both TOF and ICR analyzers. The molecular modeling results from the ammonium complex appeared to contradict the experimental results. The ammonium complex [**C6A-Et**:NH_4]$^+$ was the most abundant signal in the mass spectra. One explanation is that the complex was kept

intact by the presence of the ester side chains that prevented the NH_4^+ from escaping. However, this should have been borne out by the calculations. Alternatively, the ammonium complex [**C6A-Et**:NH_4]$^+$ may have been formed in high abundances due to the high availability of NH_4^+. The decay of the ion population after laser desorption leaves a stable component that is still relatively abundant.

The presence of amino acid adducts of derivatized calix[6]arene indicates strong non-covalently bound complexes that withstand even the MALDI process. There have been numerous attempts in this laboratory and elsewhere to form non-covalent complexes of small molecules with MALDI, such as inclusion complexes of cyclodextrins, with no success. Similarly, there have been no reports of crown ethers with ammonium or amino acids formed by MALDI. However, there are numerous reports of crown ethers and cyclodextrins forming complexes with amino acids using ESI [44–50]. ESI typically imparts less internal energy to the ion. The results in this report suggest that the complexes in the present study are significantly stronger than the corresponding inclusion complexes of cyclodextrins and crown ethers.

It has been proposed that in order to develop more powerful receptors, calixarenes should have rigid cone conformations [51]. For this reason, past research has focused mainly on the more rigid calix[4]arenes. However, gas-phase data indicates that derivatized calix[6]arenes complex amino acids more strongly than the corresponding calix[4]arene derivatives. This suggests that size, more than rigidity or the cone-like shape, is important for increasing the strength of the interaction between the amino acid and the host. In solution, the cation-π interactions are sufficient to produce long-lived complexes. These complexes, however, do not persist during MALDI ionization. Hydrogen bonds involving the ammonium hydrogens and the phenolic oxygens of the host are significantly stronger, but these interactions are more difficult to achieve in the native calix[4]arene and **C4A-Et** because of the small cavity size. Calix[6]arene and **C6A-Et** are more flexible and lack the conical structure typically favored for a host. However, molecular modeling calculations with **C6A-Et** predict that the phenolic oxygens become more available to the protonated amino acid. In addition, coordination of the protonated amino acid to these molecules fixes the conformation of the host, thereby creating the rigidity that is desired.

Native calix[6]arene does not form amino acid complexes due to extensive intramolecular hydrogen bonding. As a caveat, the mere abundance of one adduct in the MALDI spectrum compared with another does not necessarily reveal the true selectivity of the calixarene host and the intrinsic stability of the complex. The resulting relative abundance of each adduct in the mass spectrum might be a reflection of ionization efficiency rather than complex stability.

Conclusion

This mass spectrometry study suggests that calix[6]arene derivatives show stronger binding of amino acids in the gas-phase than calix[4]arenes. To the best of our knowledge, this is the first time a non-covalent complex between a calixarene and an amino acid has been observed in the gas-phase using MALDI ionization. Adducts were observed using both FT-ICR and TOF detection. The complex formation observed under MALDI conditions suggests that the modified calix[6]arenes can act as effective amino acid receptors. Efforts to investigate the behavior of these compounds in ESI experiments are currently underway in our laboratory.

Derivatized calix[6]arenes may be more effective receptors for amino acids in the gas-phase than the more commonly studied calix[4]arenes. Besides amino acids, the esters of calix[6]arene also formed complexes with ethyl and propyl amine as well as with guanidine and creatinine. The latter two compounds produced the strongest signals with the calix[6]arene esters suggesting a use for calix[6]arene derivatives as potential guanidine sensors.

Acknowledgments

The authors gratefully acknowledge funding provided by the National Science Foundation.

References

1. Lumetta, G. J.; Rogers, R. D.; Gopalan, A. S. *Calixarenes for Separations*; The American Chemical Society: Washington, D.C., 2000.
2. Gutsche, C. D. *Calixarenes Revisited*; The Royal Society of Chemistry, Letchwork, UK; 1998.
3. Vicens, J.; Boehmer, V. *Topics in Inclusion Science, Vol. III. Calixarenes: A Versatile Class of Macrocyclic Compounds*; Kluwer Academic Publishers, Dordrecht, The Netherlands, 1991.
4. Asfari, Z.; Boehmer, V.; Harrowfield, J.; Vicens, J. *Calixarenes 2001*; Kluwer Academic Publishers, Dordrecht, The Netherlands, 2001.
5. Cadogan, F.; Nolan, K.; Diamond, D. Sensor Applications (of Calixarenes). In *Calixarenes 2001*; Kluwer Academic Publishers, Dordrecht, The Netherlands, 2001; pp 627–641.
6. Rusin, O.; Kral, V. 1,1'-Binaphthyl Subunits as Recognition Groups of Novel Macrocyclic Ligands; Application for Saccharide Sensing. *Sens. Actuators B* **2001,** *B76,* 331–335.
7. Diamond, D.; Nolan, K. Calixarenes: Designer Ligands for Chemical Sensors. *Anal. Chem.* **2001,** *73,* 22A–29A.
8. Beer, P. D.; Cooper, J. B. Calixarene based anion receptors. In *Calixarenes in Action*, Mandolini, L.; Ungaro, R. (Eds.), Imperial College Press, London, UK, 2000; pp 111–143.
9. Ikeda, A.; Shinkai, S. Novel Cavity Design Using Calix[n]arene Skeletons: Toward Molecular Recognition and Metal Binding. *Chem. Rev.* **1997,** *97,* 1713–1734.
10. Cacciapaglia, R.; Mandolini, L. Calixarene Based Catalytic Systems. In *Calixarenes in Action*, Mandolini, L., Ungaro, R. (Eds.), Imperial College Press, London, UK, 2000; pp 241–264.
11. Chen, S.-H. Study of Enzyme Models and Imitation of Enzyme Action. *Chin. J. Chem.* **1999,** *17,* 309–318.
12. Perrin, R.; Harris, S. Industrial Applications of Calixarenes. *Top. Inclusion Sci.* **1991,** *3,* 235–259.

13. Shinkai, S. Functionalized Calixarenes: New Applications as Catalysts, Ligands, and Host Molecules. *Top. Inclusion Sci.* **1991,** *3,* 173–198.
14. Swager, T. M.; Xu, B. Liquid Crystalline Calixarenes. *J. Inclusion Phenom. Mol. Recognit. Chem.* **1994,** *19,* 389–398.
15. Selkti, M.; Tomas, A.; Coleman, A. W.; Douteau-Guevel, N.; Nicolis, I.; Villain, F.; de Rango, C. The First Example of a Substrate Spanning the Calix[4]arene Bilayer: The Solid State Complex of p-Sulfonatocalix[4]arene with L-Lysine. *Chem. Commun.* **2000**, *2*, 161–162.
16. Douteau-Guevel, N.; Coleman, A. W.; Morel, J.-P.; Morel-Desrosiers, N. Complexation of the Basic Amino Acids Lysine and Arginine by Three Sulfonatocalix[*n*]arenes (n = 4, 6, and 8) in Water: Microcalorimetric Determination of the Gibbs Energies, Enthalpies, and Entropies of Complexation. *J. Chem. Soc. Perkin Trans. 2* **1999**, *3*, 629–634.
17. Douteau-Guevel, N.; Coleman, A. W.; Morel, J.-P.; Morel-Desrosiers, N. Complexation of Basic Amino Acids by Water-Soluble Calixarene Sulfonates as a Study of the Possible Mechanisms of Recognition of Calixarene Sulfonates by Proteins. *J. Phys. Org. Chem.* **1998,** *11,* 693–696.
18. Antipin, I. S.; Stoikov, I. I.; Pinkhassik, E. M.; Fitseva, N. A.; Stibor, I.; Konovalov, A. I. Calix[4]arene based α-Aminophosphonates: Novel Carriers for Zwitterionic Amino Acids Transport. *Tetrahedron Lett.* **1997,** *38,* 5865–5868.
19. Arena, G.; Contino, A.; Gulino, F. G.; Magri, A.; Sansone, F.; Sciotto, D.; Ungaro, R. Complexation of native L-α-Amino Acids by Water Soluble Calix[4]arenes. *Tetrahedron Lett.* **1999,** *40,* 1597–1600.
20. Buschmann, H.-J.; Mutihac, L.; Jansen, K. Complexation of Some Amine Compounds by Macrocyclic Receptors. *J. Inclusion Phenom. Macrocyclic Chem.* **2001,** *39,* 1–11.
21. Ludwig, R. Calixarenes in Analytical and Separation Chemistry. *Fresenius J. Anal. Chem.* **2000,** *367,* 103–128.
22. Harrowfield, J. M.; Richmond, W. R.; Sobolev, A. N.; White, A. H. Alkylammonium Cation Interactions with Calixarene Anions. Part 2. Structural Characterization of a Salt of 2:3 Cation: Calixarene Stoichiometry. *J. Chem. Soc. Perkin Trans. 2* **1994**, *1*, 5–9.
23. Arena, G.; Contino, A.; Magri, A.; Sciotto, D.; Spoto, G.; Torrisi, A. Strategies Based on Calixcrowns for the Detection and Removal of Cesium Ions from Alkali-Containing Solutions. *Ind. Eng. Chem. Res.* **2000,** *39,* 3605–3610.
24. Glennon, J. D.; Horne, E.; Hall, K.; Cocker, D.; Kuhn, A.; Harris, S. J.; McKervey, M. A. Silica-Bonded Calixarenes in Chromatography. II. Chromatographic Retention of Metal Ions and Amino Acid Ester Hydrochlorides. *J. Chromatogr. A* **1996,** *731,* 47–55.
25. Araki, K.; Inada, K.; Shinkai, S. Chiral Recognition of α-Amino Acid Derivatives with a Homooxacalix[3]arene: Construction of a Pseudo-C2-Symmetrical Compound from a C3-Symmetrical Macrocycle. *Angew. Chem. Int. Ed. Engl.* **1996,** *35,* 72–74.
26. Kubo, Y.; Maeda, S. Y.; Tokita, S.; Kubo, M. Colorimetric Chiral Recognition by a Molecular Sensor. *Nature* **1996,** *382,* 522–524.
27. Arduini, A.; Cantoni, M.; Graviani, E.; Pochini, A.; Secchi, A.; Sicuri, A. R.; Ungaro, R.; Vincenti, M. Gas-Phase Complexation of Neutral Molecules by Upper Rim Bridged Calix[4]arenes. *Tetrahedron* **1995,** *51,* 599–606.
28. Vincenti, M. Host–guest Chemistry in the Mass Spectrometer. *J. Mass Spectrom.* **1995,** *30,* 925–939.
29. Regnouf-De-Vains, J.-B.; Berthalon, S.; Lamartine, R. Electrospray Mass Spectrometric Evidence of Calixarene p-Quinone Methide Formation. *J. Mass Spectrom.* **1998,** *33,* 968–970.
30. Linnemayr, K.; Allmaier, G. Ultraviolet Laser Desorption Ionization Mass Spectrometry of Selected Calixarenes with and without Matrix Assistance. *Eur. Mass Spectrom.* **1997,** *3,* 141–149.
31. Goolsby, B. J.; Brodbelt, J. S.; Adou, E.; Blanda, M. Determination of Alkali Metal Ion Binding Selectivities of Calixarenes by Matrix-Assisted Laser Desorption Ionization and Electrospray Ionization in a Quadrupole Ion Trap. *Int. J. Mass Spectrom.* **1999,** *193,* 197–204.
32. Blanda, M. T.; Farmer, D. B.; Brodbelt, J. S.; Goolsby, B. J. Synthesis and Alkali Metal Ion Binding Properties of Two Rigid Stereochemical Isomers of Calix[6]arene Bis-crown-4. *J. Am. Chem. Soc.* **2000,** *122,* 1486–1491.
33. Lippmann, T.; Wilde, H.; Pink, M.; Schaefer, A.; Hesse, M.; Mann, G. Host–Guest Complexes Between Resorcinol-Derived Calix[4]arenes and Alkylammonium Ions. *Angew. Chem.* **1993,** *105,* 1258–1260 (See also *Angew. Chem. Int. Ed. Engl.* **1993**, 1232 and 1195–1257).
34. Wong, P. S. H.; Yu, X.; Dearden, D. V. Complexes of p-Tert-Butylcalix[4]arene with Mono- and Dipositive Cations in the Gas Phase. *Inorg. Chim. Acta* **1996,** *246,* 259–265.
35. Vincenti, M.; Minero, C.; Pelizzetti, E.; Secchi, A.; Dalcanale, E. Host–Guest Chemistry in the Gas Phase and at the Gas-Solid Interface: Fundamental Aspects and Practical Applications. *Pure Appl. Chem.* **1995,** *67,* 1075–1084.
36. Vincenti, M.; Irico, A.; Dalcanale, E. Host–Guest Interactions in Mass Spectrometry. *Adv. Mass Spectrom.* **1998**, *14,* 129–150.
37. Wang, B. H.; Biemann, K. Matrix-Assisted Laser Desorption/Ionization Time-of-Flight Mass Spectrometry of Chemically Modified Oligonucleotides. *Anal. Chem.* **1994,** *66,* 1918–1924.
38. Arnaud-Neu, F.; Collins, E. M.; Deasy, M.; Ferguson, G.; Harris, S. J.; Kaitner, B.; Lough, A. J.; McKervey, M. A.; Marques, E.; Ruhl, B. L.; Schwing-Weill, M. J.; Seward, E. M. Synthesis, X-ray Crystal Structures, and Cation-Binding Properties of Alkyl Calixaryl Esters and Ketones, a New Family of Macrocyclic Molecular Receptors. *J. Am. Chem. Soc.* **1989,** *111,* 8681–8691.
39. Grady, T.; Harris, S. J.; Smyth, M. R.; Diamond, D.; Hailey, P. Determination of the Enantiomeric Composition of Chiral Amines Based on the Quenching of the Fluorescence of a Chiral Calixarene. *Anal. Chem.* **1996,** *68,* 3775–3782.
40. Cancilla, M. T.; Wong, A. W.; Voss, L. R.; Lebrilla, C. B. Fragmentation Reactions in the Mass Spectrometry Analysis of Neutral Oligosaccharides. *Anal. Chem.* **1999,** *71,* 3206–3218.
41. Tseng, K.; Hedrick, J. L.; Lebrilla, C. B. Catalog-Library Approach for the Rapid and Sensitive Structural Elucidation of Oligosaccharides. *Anal. Chem.* **1999,** *71,* 3747–3754.
42. Cancilla, M. T.; Penn, S. G.; Lebrilla, C. B. Alkaline Degradation of Oligosaccharides Coupled with Matrix-Assisted Laser Desorption/Ionization Fourier Transform Mass Spectrometry: A Method for Sequencing Oligosaccharides. *Anal. Chem.* **1998,** *70,* 663–672.
43. Tseng, K.; Lindsay, L. L.; Penn, S.; Hedrick, J. L.; Lebrilla, C. B. Characterization of Neutral Oligosaccharide-Alditols from Xenopus laevis Egg Jelly Coats by Matrix-Assisted Laser Desorption Fourier Transform Mass Spectrometry. *Anal. Biochem.* **1997,** *250,* 18–28.
44. Sawada, M.; Takai, Y.; Yamada, H.; Nishida, J.; Kaneda, T.; Arakawa, R.; Okamoto, M.; Hirose, K.; Tanaka, T.; Naemura, K. Chiral Amino Acid Recognition Detected by Electrospray Ionization (ESI) and Fast Atom Bombardment (FAB) Mass Spectrometry (MS) Coupled with the Enantiomer-Labeled (EL) Guest Method. *J. Chem. Soc. Perkin Trans. 2* **1998**, 3, 701–710.
45. Wilson, S. R.; Wu, Y. Applications of Electrospray Ionization Mass Spectrometry to Neutral Organic Molecules Including Fullerenes. *J. Am. Soc. Mass Spectrom.* **1993,** *4,* 596–603.
46. Cheng, Y.; Hercules, D. M. Measurement of Chiral Complexes of Cyclodextrins and Amino Acids by Electrospray Ionization Time-of-Flight Mass Spectrometry. *J. Mass Spectrom.* **2001,** *36,* 834–836.
47. Ramirez, J.; Ahn, S.; Grigorean, G.; Lebrilla, C. B. Evidence for the Formation of Gas-Phase Inclusion Complexes with Cyclodextrins and Amino Acids. *J. Am. Chem. Soc.* **2000,** *122,* 6884–6890.

48. Ramirez, J.; He, F.; Lebrilla, C. B. Gas-Phase Chiral Differentiation of Amino Acid Guests in Cyclodextrin Hosts. *J. Am. Chem. Soc.* **1998,** *120,* 7387–7388.
49. Prokai, L.; Ramanathan, R.; Nawrocki, J.; Eyler, J. Electrospray Ionization Mass Spectrometry of Cyclodextrin Complexes of Amino Acids and Peptides. *J. Inclusion Phenom. Mol. Recognit. Chem.* **1996,** *25,* 117–120.
50. Ramanathan, R.; Prokai, L. Electrospray Ionization Mass Spectrometric Study of Encapsulation of Amino Acids by Cyclodextrins. *J. Am. Soc. Mass Spectrom.* **1995,** *6,* 866–871.
51. Arnaud-Neu, F.; Fuangswasdi, S.; Notti, A.; Pappalardo, S.; Parisi, M. F. Calix[5]arene-Based Molecular Vessels for Alkylammonium Ions. *Angew. Chem. Int. Ed.* **1998,** *37,* 112–114.